JOURNAL OF SOLID STATE CHEMISTRY **128,** 73–79 (1997)
ARTICLE NO. SC967151

Microcalorimetric Studies of Surface Acid/Base Properties of Magnesium–Iron Catalysts Prepared from Hydrotalcite-Type Precursors

Mai Tu, Jianyi Shen[1], and Yi Chen

Department of Chemistry, Nanjing University, Nanjing 210093, China

Received June 14, 1996; in revised form September 6, 1996; accepted September 10, 1996

Magnesium–iron mixed oxides with Mg/Fe molar ratios 1, 3, and 6 were prepared from hydrotalcite-type precursors. Microcalorimetric adsorption of NH_3 and CO_2 showed that the surface acidity and basicity of the mixed oxides after calcination at 673 K are similar despite the different Mg/Fe ratios. Increasing calcination temperature from 673 to 773 K significantly decreased the surface area of the 3 Mg/Fe oxide, but the densities of both the acid and base sites were not changed. Mössbauer spectroscopy revealed that the reduction of the 3 Mg/Fe oxide (Fe_2O_3/MgO) in H_2 at 673 K converted all Fe^{3+} to Fe^{2+}. The resulted FeO/MgO exhibited the same acidity as that of the Fe_2O_3/MgO, but the basicity of the FeO/MgO was greatly enhanced. Reduction at 773 K resulted in the formation of 76% Fe^{2+} and 24% Fe^0 as detected by Mössbauer spectroscopy. The Fe/FeO/MgO sample formed exhibited very low heat for the adsorption of NH_3 (40 kJ/mol) indicating that all iron atoms on the surface are Fe^0. However, a substantial basicity remained on the surface of this sample that may account for its high olefin selectivity compared with pure iron catalyst in the Fischer–Tropsch synthesis. © 1997 Academic Press

INTRODUCTION

A complete description of a solid acid or base requires the determination of the nature as well as the strength and number of sites on the surface (1). Infrared spectroscopy is an effective technique used for identifying the nature of acid and base sites when probe molecules such as ammonia and carbon dioxide are adsorbed (2, 3). There are several methods employed in the determination of strength and number of acid/base sites (4). The technique of microcalorimetric adsorption of probe molecules has the advantage compared to the Hammet indicator and temperature-programmed desorption in that it provides much more accurately the values of strength and number of acid/base sites on solids (5). The calorimetric technique measures the strength of surface sites in terms of the bond strength formed between the sites and probe molecules, which is defined as the differential adsorption heat versus adsorbate coverage. In recent years, the acid–base properties of unsupported and supported single metal oxides have been studied by the technique of microcalorimetric adsorption (6–12). However, the similar study on mixed binary metal oxides has been seldom reported. In this paper, we present some new results obtained with the microcalorimetry on the surface acid/base properties of Mg–Fe binary oxides.

The Mg–Fe mixed oxides were prepared from their corresponding hydrotalcite-type compounds. The studies of hydrotalcite-like compounds (HTLC) used for precursors of catalysts and catalyst supports have recently attracted much attention (12–23). In a previous paper (24), we studied the synthesis and structures of Mg–Fe HTLC with Mg/Fe molar ratios from 1 to 10. The Fe/FeO/MgO catalysts resulting from the reduction of hydrotalcite precursors exhibited much higher olefin selectivity in the Fischer–Tropsch synthesis than the pure iron sample reduced from Fe_2O_3. The high olefin selectivity might result from the basicity of MgO in the catalysts. Thus, we focused our studies in this work on the surface acid/base properties of Mg–Fe binary oxides and the FeO/MgO and Fe/FeO/MgO catalysts obtained from the Mg–Fe hydrotalcite precursors.

EXPERIMENTAL

The preparation of magnesium hydroxide, ferric hydroxide, and Mg–Fe HTLC samples with Mg/Fe molar ratios 1, 3, and 6 was described in our previous paper (24). After calcination at 673 K, these precursors were converted into corresponding oxides. The Mg–Fe Oxide samples were designated as *n*Mg/Fe according to their molar ratios. The 3Mg/Fe sample was further treated to obtain the surfaces with different properties. Specifically, the sample was calcined at 773 K to see the effect of surface area on the surface acid–base properties. The sample was also reduced in H_2 for

---

[1] To whom correspondence should be addressed.

0022-4596/97 $25.00

4 h at 673 and 773 K, respectively, to obtain different iron phases. X-ray diffraction (XRD) was performed to determine the phases of the samples before and after calcination. The apparatus employed is a Shimadzu XD-3A X-ray diffractometer using an iron target with a graphite monochromator. The wavelength was Fe$K\alpha = 0.19373$ nm. The surface areas of the samples were measured by N_2 adsorption at 77 K using the BET method. Mössbauer spectroscopy was used to monitor the iron species in the samples treated at different conditions. In particular, the samples were reduced in H_2 in an *in situ* cell which allows the samples to be detected with Mössbauer spectroscopy without exposure to air. All the spectra were collected at room temperature by using a constant acceleration spectrometer equipped with a ^{57}Co/Pd source. The velocity scale of the spectrometer was calibrated with the ^{57}Fe Mössbauer resonance. Isomer shifts are reported relative to α-Fe. All iron species are assumed to have the same recoilless fraction to calculate the relative amount of different iron phases in the samples according to their relative peak areas.

Microcalorimetric measurements of the adsorption of ammonia and carbon dioxide were carried out by using a Tian–Calvet heat-flow microcalorimeter (25). The apparatus was linked to a gas-handling and volumetric adsorption system equipped with a Baratron pressure sensor (MKS) for precision pressure measurements. Heat-flow signals were detected by transducer assemblies manufactured by ITI. The differential heat of adsorption versus adsorbate coverage was determined by measuring the heats evolved when doses of gas (1–2 μmol per dose) were introduced sequentially onto the sample until the final equilibrium pressure reached 650 Pa. Ammonia and carbon dioxide (purity $> 99.9\%$) were purified by successive freeze–pump–thaw cycles. Before microcalorimetric measurements, the oxide samples were usually dried under vacuum at 573 K for 1 h, calcined at 673 K for 4 h, and finally evacuated at 673 K for 2 h. The reduction of the samples was performed in the calorimeter in H_2 with the same conditions as for the Mössbauer determination, followed by evacuation at 673 K for 2 h before microcalorimetric measurements. All the microcalorimetric measurements were performed at 423 K.

RESULTS AND DISCUSSION

All the Mg–Fe samples prepared before calcination exhibited the typical XRD patterns of the hydrotalcite structure as described in the previous paper (24). The XRD patterns of the Mg–Fe samples after calcination are shown in Fig. 1. The only phase detected for the samples of 3Mg/Fe and 6Mg/Fe calcined at 673 K or 773 K is MgO with the main peaks at the *d* values of 1.49, 2.11, and 2.43 (26). However, the 1Mg/Fe sample displays a peak with the *d* value at 2.55 besides the diffraction pattern of MgO, which may be attributed to the phase of spinel $MgFe_2O_4$ (27). These results demonstrate that the mixed oxide samples may mainly possess a brucite-like structure with Fe^{3+} randomly distributed in the octahedral sites owing to the similar ionic radii of about 0.065 nm for Fe^{3+} and Mg^{2+} cations. The 3Mg/Fe sample exhibited more intensive diffraction lines when it was calcined at 773 K than when it was calcined at 673 K, indicating the greater crystallite size of the sample calcined at the higher temperature.

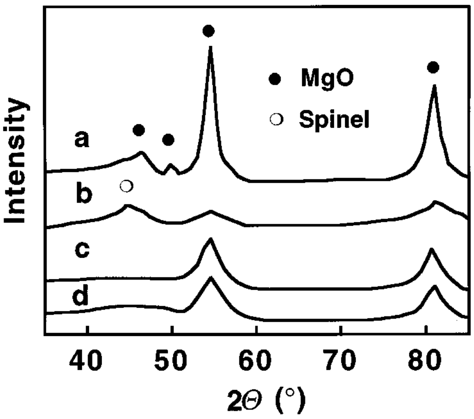

FIG. 1. X-ray diffraction patterns of the Mg–Fe mixed oxides obtained from Mg–Fe hydrotalcites. The samples and calcination temperatures are (a) 3Mg/Fe (773 K), (b) 1Mg/Fe (673 K), (c) 3Mg/Fe (673 K), (d) 6Mg/Fe (673 K).

The BET areas of the samples are given in Table 1. The Mg–Fe mixed oxides exhibited similar large specific surface areas, around 200 m^2/g, after calcination at 673 K. When the 3Mg/Fe sample was calcined at 773 K, the surface area decreased to 116 m^2/g, corresponding to the increase of the sample in crystallite size as indicated by the XRD results above. The surface areas decreased to 39 and 21 m^2/g after the 3Mg/Fe sample was reduced at 673 and 773 K, respectively.

In Fig. 2 are shown plots of the differential heat of ammonia adsorption as a function of adsorbate coverage on the oxide samples calcined at 673 K. Fe_2O_3 displays the strongest acidity in terms of both initial heat and coverage for the adsorption of ammonia: the initial heat is about 115 kJ/mol and the saturation coverage is about 3.5 $\mu mol/m^2$. In addition, the heat versus coverage curve displays a plateau with the adsorption heat between 100 and 120 kJ/mol. In contrast, the MgO sample only presents very few and weak acid sites: the initial differential heat of ammonia adsorption is around 55 kJ/mol and the coverage is negligible. The mixed Mg–Fe oxides exhibited intermediate acidity compared to the Fe_2O_3 and MgO in terms of the strength and saturation coverage for the adsorption of ammonia. It is interesting to note that the 3Mg/Fe and 6Mg/Fe samples displayed exactly the same adsorption heat versus coverage curves: the initial heat is about 100 kJ/mol and the saturation coverage of ammonia is about 1.2 $\mu mol/m^2$. This

TABLE 1

The BET Areas and Mössbauer Results for the Mg–Fe Mixed Oxide Samples as Well as for the Reference Oxides MgO and Fe_2O_3

Sample	Treatment	BET surface area (m^2/g)	Mössbauer iron phase assignments
MgO	673 K calcination	262	—
Fe_2O_3	673 K calcination	37	—
1Mg/Fe[a]	673 K calcination	200	—
3Mg/Fe[a]	673 K calcination	218	100% Fe^{3+}
	773 K calcination	116	—
	673 K reduction	39	100% Fe^{2+}
	773 K reduction	21	76% Fe^{2+}, 24% Fe^0
6Mg/Fe[a]	673 K calcination	203	—

[a] The Mg–Fe samples are designated as *n*Mg/Fe according to their molar ratios.

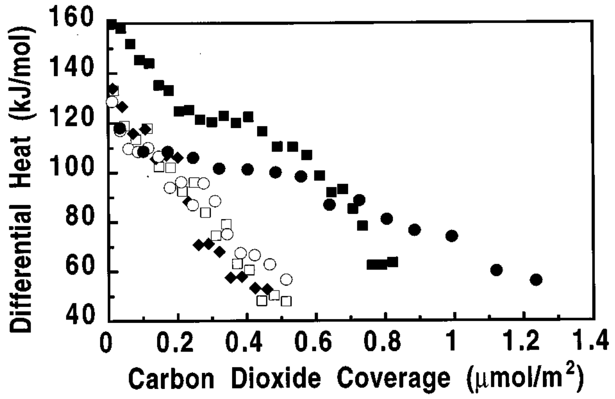

FIG. 3. Differential heat versus carbon dioxide coverage at 423 K on MgO (■), 6Mg/Fe (□), 3Mg/Fe (◆), 1Mg/Fe (○), and Fe_2O_3 (●) calcined at 673 K.

indicates that the two samples might possess the same surface structure. The 1Mg/Fe samples showed a little higher adsorption heat in the entire ammonia coverage than the 3Mg/Fe and 6Mg/Fe samples, which may be caused by the formation of the spinel phase in the 1Mg/Fe sample.

Figure 3 presents the curves of the differential heat of carbon dioxide adsorption as a function of the coverage on the oxide samples. MgO displays the strongest basicity with initial heat of about 160 kJ/mol and saturation coverage of about 0.8 μmol/m² for the adsorption of carbon dioxide. The plots of the differential heat for the three mixed Mg–Fe oxides showed the similar trend: the differential heat decreased from 130 to about 50 kJ/mol with the increase of carbon dioxide coverage to about 0.5 μmol/m². Fe_2O_3 exhibited the lowest initial heat for the adsorption of carbon dioxide. However, the sample had the largest amount of the base sites. The saturation coverage of carbon dioxide on this sample was as high as 1.2 μmol/m², even higher than that on MgO. This may reflect the fact that the unsaturated oxygen anions, which are the Lewis base sites that adsorb carbon dioxide, may be denser on Fe_2O_3 than the MgO. In contrast to ammonia adsorption, for which both the initial heats and saturation coverage on the Mg–Fe samples were in between those on Fe_2O_3 and MgO, the saturation coverage of carbon dioxide on the Mg–Fe mixed oxides was lower than that on the Fe_2O_3 and MgO samples, although the initial heats for the adsorption of carbon dioxide on these samples were between those on Fe_2O_3 and MgO. The similarity of the bulk structure of the Mg–Fe samples to that of MgO, as evidenced by the XRD results, may explain the lower coverage for carbon dioxide adsorption on the Mg–Fe samples than on MgO. On the other hand, the incorporation of Fe^{3+} in the structure of MgO in the Mg–Fe samples may result in decreased basicity of these samples compared to MgO.

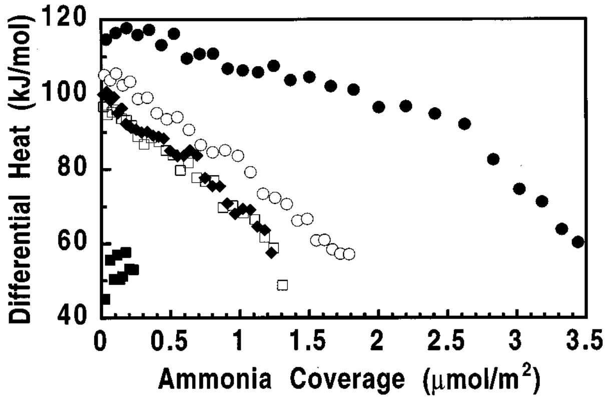

FIG. 2. Differential heat versus ammonia coverage at 423 K on MgO (■), 6Mg/Fe (□), 3Mg/Fe (◆), 1Mg/Fe (○), and Fe_2O_3 (●) calcined at 673 K.

A better view of the acid–base site energy distributions is shown in the following two histograms. These histograms were plotted by fitting the curves of differential heat versus coverage by polynomials and then using the fitted polynomials to determine the number of adsorbates that interact with the differential heat within a given range of coverage.

Figure 4 shows the strength distributions of the acid sites of the oxide samples calcined at 673 K. The acidic sites on Fe_2O_3 for the adsorption of ammonia are mainly distributed in the range from 60 to 120 kJ/mol. The most populated sites on Fe_2O_3 have a strength of about 110 kJ/mol. MgO possesses very few sites with differential heat for ammonia adsorption lower than 60 kJ/mol. In contrast, the population of Mg–Fe samples mostly have acid sites at the strength with differential heat around 90 kJ/mol.

Figure 5 represents the basic site energy distributions of oxide samples calcined at 673 K. Fe_2O_3 possesses base sites with heats from 50 to 120 kJ/mol, in which a great part (about 0.33 μmol/m²) are around 105 kJ/mol, corresponding to the plateau of CO_2 adsorption sites shown in Fig. 3.

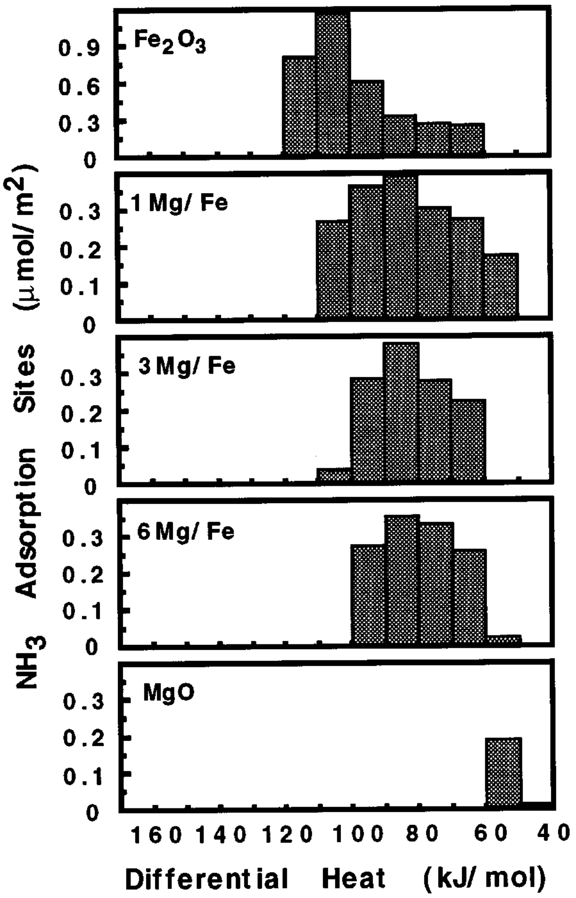

FIG. 4. Histograms of the distribution of interaction strengths for ammonia adsorption on the oxide samples calcined at 673 K.

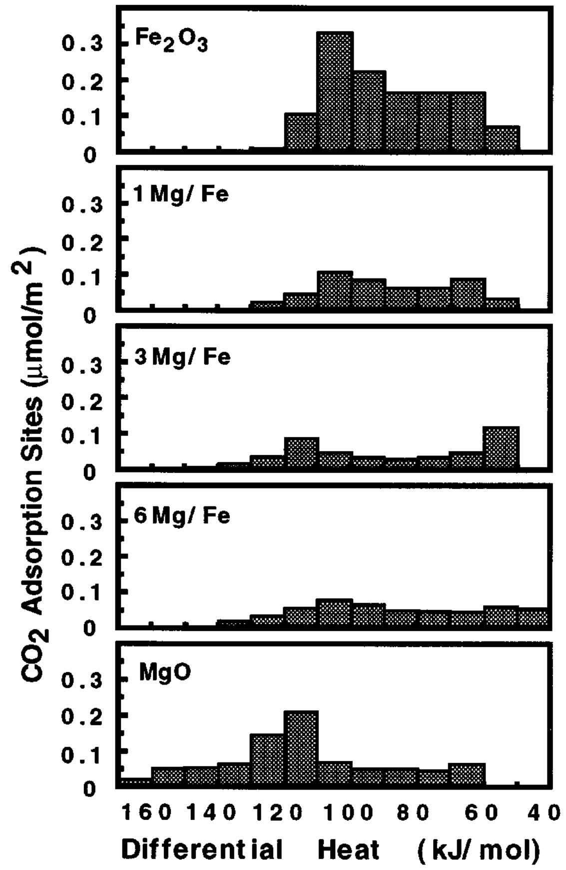

FIG. 5. Histograms of the distribution of interaction strengths for carbon dioxide adsorption on the oxide samples calcined at 673 K.

The MgO is the only sample studied in this work that possesses base sites stronger than 150 kJ/mol. However, the most populated base sites on MgO are around 120 kJ/mol. Finally, the histograms in Fig. 5 show that mixed oxide samples exhibit a similar homogeneous distribution for base sites in the range between 140 to 50 kJ/mol.

Next, we consider the effect of calcination temperature on the surface acid–base properties of Mg–Fe mixed oxides. The 3Mg/Fe sample is used as an example. In Fig. 6 are shown the results of microcalorimetric adsorption of ammonia and carbon dioxide on the 3Mg/Fe sample calcined at 673 and 773 K. It is seen that in each case, the sample has more acid sites than base sites, but the acid sites are much weaker than the base sites in terms of the initial adsorption heats. However, Fig. 6a shows that the sample calcined at 673 K has more and stronger sites for both acid and base sites than the sample calcined at the higher temperature. This is seen from the conventional view point because the coverage in Fig. 6a is expressed in the unit μmol/g. When the coverage is divided by the surface area, we see the interesting results shown in Fig. 6b: both the acid and base sites have the same strength distribution for samples calcined at different temperatures. These results demonstrate that the concentration of either acid or base sites on the surface, as well as the surface structure, may be the same for samples calcined at different temperatures. The only difference is the decrease of the surface area when the sample is calcined at the higher temperature, which causes the decrease of total acid and base sites per gram of the sample. Apparently, the two units used for adsorption coverage sometimes cause confusion about the strengths of solid acids and bases. We therefore suggest that these two cases be differentiated by defining the term *specific strength distribution* for solid acid and base sites when the coverage is expressed in number of sites per square meter. Finally, we should point out that the comparison between the strength distribution and the *specific strength distribution* for samples with the same composition may provide useful information about the variation of the surface structures.

The effect of reduction treatment on the surface properties was also investigated by first monitoring the iron phase variations in the 3Mg/Fe sample using Mössbauer

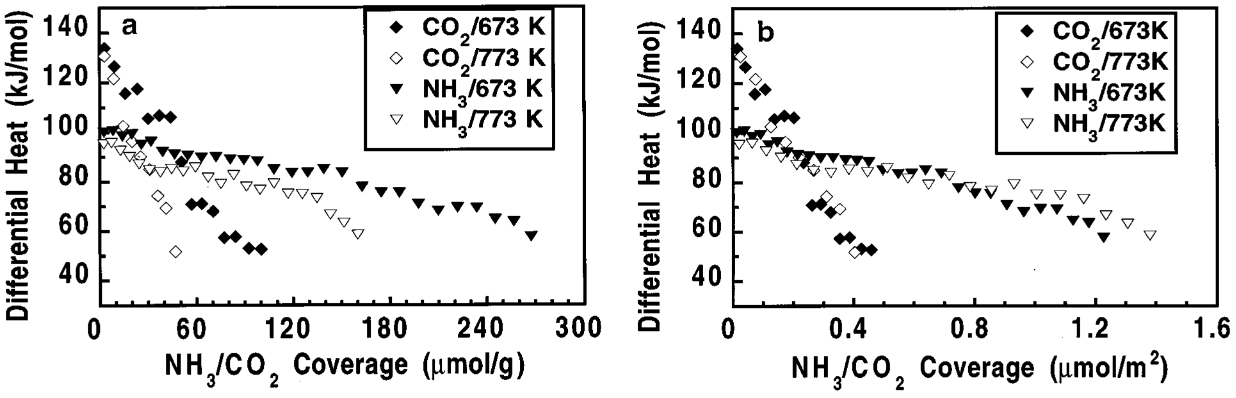

FIG. 6. Microcalorimetric adsorption of NH_3 and CO_2 at 423 K on the 3Mg/Fe sample calcined at 673 and 773 K as indicated in the legends.

spectroscopy. The sample after calcination at 673 K displayed a doublet with isomer shift 0.28 mm/s and quadruple splitting of 0.67 mm/s, characteristic of Fe^{3+} (Fig. 7a). This indicates that Fe^{3+} cations were highly dispersed in the lattice of MgO, consistent with the XRD results discussed above. Upon reduction in H_2 at 673 K, the sample gave a spectrum exhibiting another doublet with isomer shift 1.01 mm/s and quadruple splitting of 0.85 mm/s characteristic of Fe^{2+}, as shown in Fig. 7b. Further reduction at 773 K resulted in the formation of metallic iron in the sample as evidenced by the appearance of a magnetically splitting sextuplet with the hyperfine field of 330 kOe. The 773 K reduced sample contained about 76% Fe^{2+} and 24% Fe^0, according to their relative spectral areas in the Mössbauer spectrum in Fig. 7c. These Mössbauer results are also summarized in Table 1. For the sake of convenience in the following discussions, we define the 3Mg/Fe sample as Fe_2O_3/MgO, FeO/MgO, and Fe/FeO/MgO as calcined at 673 K, and reduced at 673 and 773 K, respectively.

The plots for the differential heats of ammonia adsorption on the 3Mg/Fe sample reduced at different temperatures are shown in Fig. 8. The result for the sample calcined a 673 K is also shown for comparison. It is noteworthy that the Fe_2O_3/MgO and FeO/MgO samples display the same trend for differential heat until the coverage reaches about 1.2 μmol/m². This implies that the two samples may have

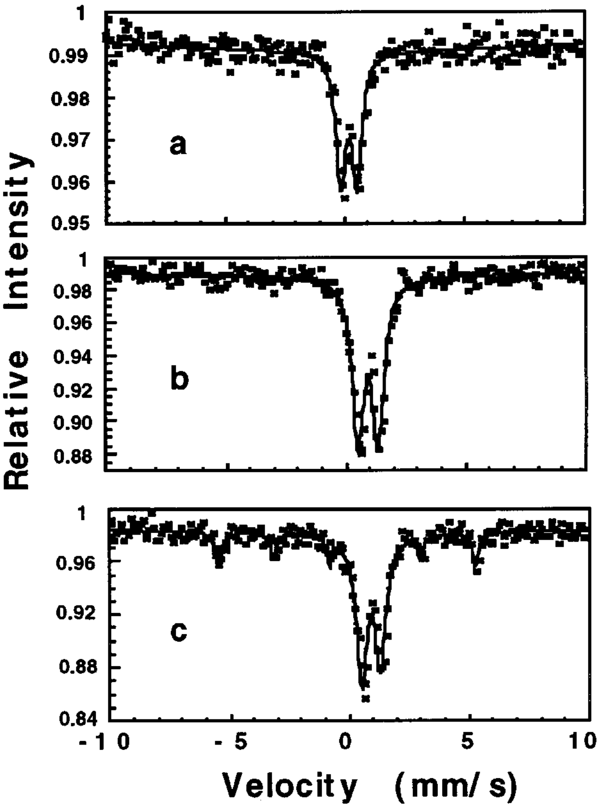

FIG. 7. Mössbauer spectra of the 3Mg/Fe sample calcined at 673 K (a) and reduced in H_2 at 673 K (b) and 773 K (c), respectively.

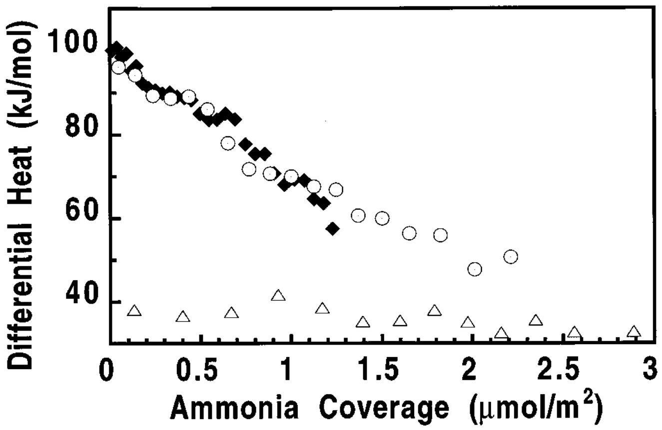

FIG. 8. Differential heat versus coverage for the adsorption of ammonia at 423 K on the 3Mg/Fe sample calcined at 673 K (◆) (Fe_2O_3/MgO), reduced at 673 K (⊙) (FeO/MgO), and reduced at 773 K (△) (Fe/FeO/MgO).

the same Sanderson electronegativity on the surface (5, 28). Furthermore, the reduction at 673 K causes an increase in the ammonia coverage, indicating that the reduction might have caused an enrichment of iron cations on the surface. The further reduction at 773 K results in a sharp decrease in differential heat for the adsorption of ammonia. Mössbauer spectroscopy has shown that this sample contained about 24% metallic iron. We suggest that the sites of iron cations on the surface of the Fe/FeO/MgO sample might have been covered by the metallic iron formed upon reduction, which would totally change the surface structure of the sample.

Since the surface electronegativities of the Fe_2O_3/MgO and FeO/MgO samples are equal, we can estimate the degree to the iron cations are enriched on the surface after the reduction at 673 K. The Sanderson electronegativities of FeO, Fe_2O_3, and MgO are 2.26, 2.46, and 2.22, respectively (29). Suppose the surface composition for the two samples is $FeO \cdot x MgO$ and $FeO_{1.5} \cdot y MgO$, respectively. With the supposition of equal electronegativities we have the equation (29):

$$(2.26 \times 2.22^{x})^{1/(1+x)} = (2.46 \times 2.22^{y})^{1/(1+y)}$$

When x is equal to 1, y is found to be 10. This calculation suggests that iron cations on the surface of FeO/MgO are greatly enriched compared with those on the Fe_2O_3/MgO sample. This enrichment may result from the migration of iron cations from the bulk to the surface upon reduction because reduction should always begin at the surface.

Figure 9 shows the microcalorimetric results for the adsorption of carbon dioxide on the Fe_2O_3/MgO, FeO/MgO, and Fe/FeO/MgO samples. It demonstrates that the reduction at 673 K significantly enhanced the adsorption for carbon dioxide. This may be because FeO is less electronegative than Fe_2O_3. In contrast to the case for the adsorption of ammonia, the Fe/FeO/MgO sample formed after reduction at 773 K adsorbed a great amount of carbon dioxide compared to the Fe_2O_3/MgO and FeO/MgO samples. This indicates that the metallic iron did not cover the oxygen anions; instead, the reduction at 773 K produced more oxygen anions on the surface for the adsorption of carbon dioxide. This may explain why this sample exhibited much higher olefin selectivity than the pure iron sample in the Fischer–Tropsch reaction (24).

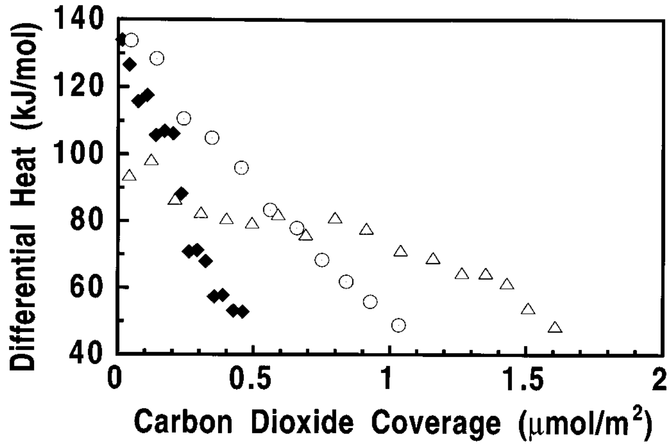

FIG. 9. Differential heat versus coverage for the adsorption of dioxide at 423 K on the 3Mg/Fe sample calcined at 673 K (◆) (Fe_2O_3/MgO), reduced at 673 K (⊙) (FeO/MgO), and reduced at 773 K (△) (Fe/FeO/MgO).

CONCLUSIONS

Microcalorimetric measurements of NH_3 and CO_2 adsorption showed that the mixed oxides with Mg/Fe ratios from 1 to 6 exhibited similar surface acidity and basicity. The density and strength of the acid sites on the mixed oxides are significantly lower than those on Fe_2O_3 but much higher than on MgO. In contrast, the initial heat of CO_2 adsorption for the mixed oxides is higher than for Fe_2O_3 but lower than for MgO. Fe_2O_3 possesses the densest acid and base sites in the oxides studied, revealing that the oxide may have more unsaturated iron cations and oxygen anions on the surface. XRD results showed that the mixed oxides exhibited a bulk structure similar to that of MgO, which may account for the lower CO_2 coverage on the mixed oxides than on Fe_2O_3 or MgO. Increasing calcination temperature from 673 to 773 K significantly decreased the surface area of the 3Mg/Fe oxide, but the densities of both acid and base sites, as well as the strength distributions, were not changed, indicating that the surface structure of the sample did not change upon calcination at the higher temperature. In such a case, microcalorimetric adsorption may become a structure-sensitive technique that can be used to probe surface variations when a sample is treated under different conditions. The 3Mg/Fe (Fe_2O_3/MgO) sample was reduced to FeO/MgO and Fe/FeO/MgO (24% Fe^0) when treated in H_2 at 673 and 773 K, respectively. Microcalorimetric adsorption of NH_3 and CO_2 revealed the enrichment of iron on the surface upon reduction, which may explain the fact that the FeO/MgO sample exhibited similar acidity to but higher basicity than the Fe_2O_3/MgO sample. The reduction of iron to Fe^0 on the surface greatly decreased the NH_3 adsorption heat while it considerably enhanced the surface base density.

ACKNOWLEDGMENTS

We acknowledge financial support from the Trans-Century Training Program Foundation for the Talents by the State Education Commission of China and the National Natural Science Foundation of China. Special thanks are extended to Professor J. A. Dumesic, Mr. B. Spiewak, Dr. B. Handy, and D. Chen in the Department of Chemical Engineering, University of Wisconsin at Madison, for their technical help in the establishment of our microcalorimeter.

REFERENCES

1. K. Tanabe, M. Misono, T. Ono, and H. Hattori, "*Studies in Surface and Catalysis*," Vol. 51, Elsevier, Amsterdam, 1989.
2. A. A. Tsyganenko, D. V. Pozdnyakov, and V. N. Filimonov, *J. Mol. Struct.* **29,** 299 (1975).
3. G. Busca and V. Lorenzelli, *Mater. Chem.* **7,** 89 (1982).
4. J. Kijenski and A. Baiker, *Catal. Today* **5,** 1 (1989).
5. N. Cardona-Martinez and J. A. Dumesic, *Adv. Catal.* **38,** 149 (1992).
6 A. Auroux and A. Gervasini, *J. Phys. Chem.* **94,** 6371 (1990).
7. Jianyi Shen, R. D. Cortright, Yi Chen, and J. A. Dumesic, *J. Phys. Chem.* **98,** 8067 (1994).
8. Jianyi Shen, M. J. Lochhed, K. L. Bray, Yi Chen, and J. A. Dumesic, *J. Phys. Chem.* **99,** 2384 (1995).
9. R. R. Gatte and J. Phillips, *J. Catal.* **16,** 49 (1989).
10. N. Cardona-Martinez and J. A. Dumesic, *J. Catal.* **125,** 427 (1990).
11. Jianyi Shen, R. D. Cortright, Yi Chen, and J. A. Dumisic, *Catal. Lett.* **26,** 247 (1994).
12. Jianyi Shen, J. M. Kobe, Yi Chen, and J. A. Dumesic, *Langmuir* **10,** 3902 (1994).
13. C. Busetto, G. Del Piero, G. Manara, F. Trifiro, and A. Vaccari, *J. Catal.* **85,** 260 (1984).
14. W. T. Reichle, *J. Catal.* **94,** 547 (1985).
15. W. T. Reichle, S. Y. Kang, and D. S. Everhardt, *J. Catal.* **101,** 352 (1986).
16. T. Yamaoka, M. Abe, and M. Tsuji, *Mater. Res. Bull.* **24,** 1183 (1989).
17. H. Schaper, J. J. Berg-slot, and W. H. Stock, *J. Appl. Catal.* **54,** 79 (1989).
18. F. Cavani, F. Trifiro, and A. Vaccari, *Catal. Today* **11,** 173 (1991).
19. O. Clause, B. Rebours, E. Merlen, F. Trifiro, and A. Vaccari, *J. Catal.* **133,** 231 (1992).
20. A. L. McKenzie, C. T. Fishel, and R. J. Davis, *J. Catal.* **138,** 547 (1992).
21. R. J. Davis and E. G. Derouane, *J. Catal.* **132,** 269 (1991).
22. A. Corma, V. Fornes, R. M. Martin-Aranda, and F. Rey, *J. Catal.* **134,** 58 (1992).
23. K. Fuda, N. Kudo, S. Kawai, and T. Matsunaga, *Chem. Lett.*, 777 (1993).
24. Jianyi Shen, Bin Guang, Mai Tu, and Yi Chen, *Catal. Today* **30,** 77 (1996).
25. B. E. Handy, S. B. Sharma, B. E. Spiewak, and J. A. Dumesic, *Measurement Sci. Technol.* **4,** 1350 (1993).
26. JCPDS Card 4-829. International Center for Diffraction Data 1987.
27. JCPDS Card 17-464. International Center for Diffraction Data 1987.
28. R. T. Sanderson, *J. Am. Chem. Soc.* **105,** 2259 (1983).
29. J. E. Huheey, "Inorganic Chemistry: Principles of Structure and Reactivity," 3rd ed., Harper & Row, New York, 1983.